Assessment of Downward Longwave Radiation Models in Clear-Sky Desert Conditions

Dunia Bachour[1], Daniel Perez-Astudillo[1], Hissa Al-Hajri[1] and Antonio Sanfilippo[1]

[1] Qatar Environment and Energy Research Institute, Hamad Bin Khalifa University, Qatar Foundation, Doha (Qatar)

Abstract

The longwave downward radiation (LDR), emitted by the atmosphere and clouds, is a crucial parameter for the determination of the radiative energy budget on the earth's surface. The direct measurement of LDR is very sensitive and requires specialized and expensive sensors, and is commonly not available at most meteorological monitoring sites, and considerable efforts have been made to determine LDR from the available atmospheric parameters of a particular site. This work presents an analysis of the longwave downward atmospheric radiation in a region of desert conditions. The performance of several downward longwave radiation models has been evaluated during clear-sky conditions, determining the more adapted empirical relation for the observed local conditions. For validation, ground measurements of LDR and atmospheric parameters were used at two different sites covering a period of several years. The statistical analysis using the original empirical coefficients of the models evaluated here shows under or over-estimation of the measured data. A local calibration was performed, retrieving the local coefficients over a period of one year, showing a decreased errors and a better statistical analysis for estimating clear-sky LDR under the local conditions of Qatar.

Keywords: longwave downward radiation, clear-sky, desert conditions, radiation budget

1. Introduction

The atmospheric longwave downward radiation (LDR) is an important parameter for the determination of the radiation budget at the earth's surface. It depends mainly on the vertical distribution of air temperature, water vapor, and the presence of aerosols and clouds in the atmospheric column within the first few kilometers above the ground.

Equation 1 shows the calculation of the net radiation budget Rn in W/m^2, including the absorption and reflection of the incoming shortwave solar radiation, as well as the longwave upward and downward radiation.

$$R_n = (1 - \alpha) * G + LDR - LUR \quad \text{(eq.1)}$$

where G is the global horizontal radiation received on the earth surface, α is the ground albedo and LUR is the longwave upper radiation emitted from the earth's surface towards the atmosphere.

Direct on-site measurements are usually the most accurate method used to obtain the long-wave downward radiation component of the atmosphere. When not available, several models exist in the literature for the estimation of the long wave downward radiation, generally based on the Stefan–Boltzmann law, and depending on the atmosphere's emissivity and the fourth power of the absolute temperature. The most accurate models are generally the numerical radiation transfer models used with the correct atmospheric input information; however, the correct input parameters are not usually available and these models are in general complex and time consuming. More simple models exist, based on empirical correlations between LDR and readily available meteorological observations, such as sunshine duration, air temperature and vapor pressure. These models are mostly developed under clear sky conditions, wherein the emissivity depends largely on the air temperature and water vapor pressure, and they are more adapted to the site where they were developed and locally calibrated.

In the present study, we evaluate 9 clear-sky models proposed in the literature to calculate the emissivity and consequently LDR, and compare it with LDR measured at ground level at two different sites in Qatar. The objective is to determine the more suitable emissivity model to the atmospheric conditions observed here, and to perform local calibration to develop local models.

doi:10.18086/eurosun.2022.15.01 Available at http://proceedings.ises.org

2. Methodology

In clear-sky conditions, LDR estimation follows the equation

$$LDR = \varepsilon * \sigma * T_a^4 \quad \text{(eq.2)}$$

where ε is the effective clear-sky emissivity of the atmosphere, σ is the Stefan Boltzmann constant and T_a is the integrated temperature over the atmospheric column above the ground that emits longwave radiation.

T_a is typically estimated from ground-based meteorological observations, and is considered here as the ambient air temperature in Kelvin.

ε is calculated with empirical equations: some of these equations consider the temperature alone such as in equations 3 (Swinbank, 1963) and 6 (Idso and Jackson, 1963), some consider the water vapor pressure e_a alone such as in equation 4 (Brunt, 1932), and some consider both T_a and e_a such as in equations 5 (Brutsaert, 1975), 7 (Idso, 1981), 8 (Sugita and Brutsaert, 1993), 9 (Duarte et al., 2006), 10 (Kruk et al., 2010), and 11 (Prata, 1996).

$$\varepsilon = 9{,}365 * 10^{-6} * {T_a}^2 \quad \text{(eq.3)}$$

$$\varepsilon = 0.52 + 0.065 * {e_a}^{1/2} \quad \text{(eq.4)}$$

$$\varepsilon = 1.24 * \frac{{e_a}^{1/7}}{T_a} \quad \text{(eq.5)}$$

$$\varepsilon = 1 - 0.261 * \exp(-0.00077 * (T_a - 273.13)^2)) \quad \text{(eq.6)}$$

$$\varepsilon = 0.7 + 5.95 * 10^{-5} * e_a * \exp(\frac{1500}{T_a}) \quad \text{(eq.7)}$$

$$\varepsilon = 0.714 * \frac{e_a^{0.0687}}{T_a} \quad \text{(eq.8)}$$

$$\varepsilon = 0.625 * \frac{e_a^{0.131}}{T_a} \quad \text{(eq.9)}$$

$$\varepsilon = 0.576 * \frac{e_a^{0.202}}{T_a} \quad \text{(eq.10)}$$

$$\varepsilon = 1 - ((1+\omega) * Exp\,(-(1.2 + 3*\omega)^{0.5})),\ \omega = 0.465 * (\frac{e_a}{T_a}) \quad \text{(eq.11)}$$

In order to determine the water vapor pressure e_a, we use the definition of the relative humidity RH and the water vapor saturation pressure calculation, following the equations by Wagne and Pruß (2002):

$$RH = \frac{e_a}{e_{as}} * 100\% \quad \text{(eq.12)}$$

$$\vartheta = 1 - \frac{T_a}{T_c} \quad \text{(eq.13)}$$

$$\ln\left(\frac{e_{as}}{e_c}\right) = \frac{T_c}{T_a} * (C_1\vartheta + C_2\vartheta^{1.5} + C_3\vartheta^3 + C_4\vartheta^{3.5} + C_5\vartheta^4 + C_6\vartheta^{7.5}) \quad \text{(eq.14)}$$

Where e_{as} is the water vapor saturation pressure, T_c and P_c are respectively the water vapor critical temperature (647.096 K) and critical pressure (220 640 hPa), and C_i are empirical coefficients.

In order to determine the clear sky conditions, we calculate a clear-sky ratio K_c as follows:

$$K_c = \frac{G}{Gc} \quad \text{(eq.15)}$$

Where G is the measured global horizontal irradiance and Gc is the clear-sky global horizontal irradiance calculated using the ESRA clear-sky model (Rigollier et al., 2000). The clear-sky conditions are those for which the clear-sky ratio is greater than 0.85.

In this study, we use the cited equations proposed in the literature to calculate the emissivity in clear-sky conditions, and then insert it into equation 2 to estimate LDR and compare it with LDR measured at ground level. All LDR and solar data are aggregated into 10-min averages in order to match the temporal resolution of the meteorological data.

3. Experimental setup

For the ground measurements of LDR two different pyrgeometers were used, a CGR4 and an MS-202, each installed at a different site (different location and conditions), with the sites located 85 km apart. The CGR4 pyrgeometer from Kipp and Zonen (highlighted with a red circle on the top right of figure 1), is part of a complete solar monitoring station installed at the rooftop of the research building of the Qatar Environment and Energy Research Institute in Doha, indicated here as site 1, measuring all the broadband solar radiation components, namely beam or direct normal (Gb), global horizontal (G) and diffuse horizontal (Gd) irradiances. The CGR4 is mounted on a sun tracker, and has a shading mechanism to prevent direct exposure to solar radiation. It also has a ventilation unit to help stabilize the dome temperature and reduce dust accumulation on the dome. An automatic weather station (AWS) is installed nearby on the same rooftop, measuring the meteorological parameters (temperature, relative humidity, pressure, and wind speed and wind direction), at 3m height from the rooftop surface. It is to be noted that the whole experimental setup described here for site 1 has been slightly relocated to another location within the same vicinity, therefore we differentiate in the data analysis between the period 2014-2017, and the period 2020-2021.

The MS-202 is installed as a standalone sensor on a horizontal platform (figure 1, bottom right) at a remote site in the desert, called here site 2. A high-quality solar monitoring station is also installed on-site, measuring G, Gb, and Gd. Few kilometers apart, an AWS is installed by the Qatar Meteorological Department and measures the meteorological components, at 10 m height from the ground. The analysed period for site 2 is for years 2020 and 2021.

Cleaning of the sensor domes and checking of the alignment of the radiation sensors are done regularly (twice a week). The solar and LDR data are collected as one-minute averages, and quality checks were applied to filter out low quality data, based on physically possible limits. The meteorological data are collected as 10-minute averages.

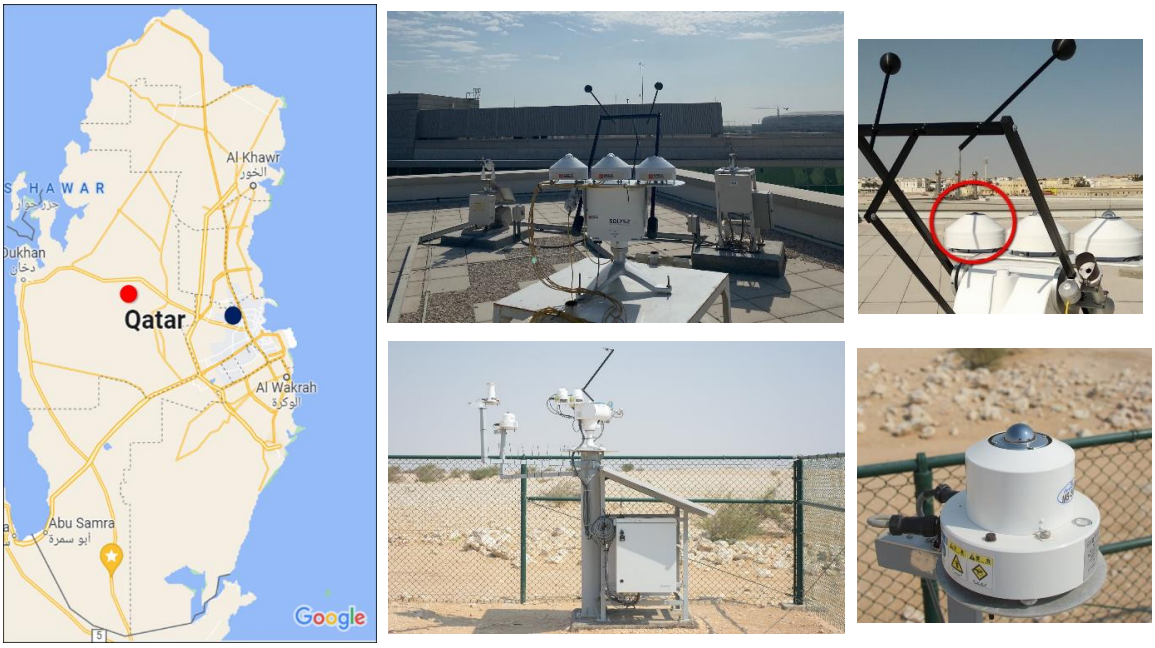

Fig. 1: Two experimental sites and two types of equipment: Kipp and Zonen station (top), EKO station (bottom).

4. Analysis and Results

For the comparison between the estimated and measured LDR, we represent the data in two-dimensional scatter plots. Figure 2 shows the scatter plot of the modeled and measured LDR at site 1 (left) and site 2 (right), using equations 4 and 3 respectively to determine the clear-sky emissivity for year 2020. The one-to-one line is indicated in red. As discussed above, the clear sky conditions are determined using the ESRA model to determine the clear-sky index. Only data with positive radiation values and solar zenith angle less than 90 degrees, and clear sky ratio higher than 0.85 are considered. The performance of the emissivity models described in equations 3 to 11 is evaluated in terms of the mean bias error (Bias) and the root mean square error (RMSE). The difference and its square between the estimated and measured LDR data at the same time stamps is calculated for a one-year period. These differences and their squares are summarized to determine the corresponding bias and root mean square error, and then expressed in relative values (rBias, rRMSE) with respect to the mean values calculated from the ground measurements. Tables

1 and 2 show the statistical parameters of the comparison between measured and estimated LDR, reporting the number of data points, the relative bias and the relative RMSE. The correlation factors were also calculated and found to be greater than 0.9 for all the comparisons considered here.

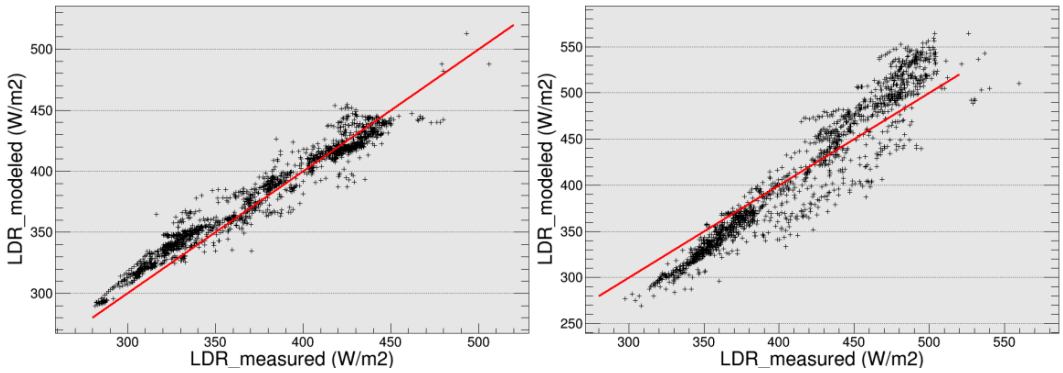

Fig. 2: Comparison between estimated and measured LDR for clear-sky conditions in year 2020. Site 1 (left). Site 2 (right).

Tab. 1: Statistical parameters for the validation of several models for estimating LDR. Site 1 (2014-2017). The lowest values are highlighted in red.

SITE 1								
Year	**2014**		**2015**		**2016**		**2017**	
Npoints	**1113**		**871**		**1862**		**1052**	
Error(%)	rBias	rRMSE	rBias	rRMSE	rBias	rRMSE	rBias	rRMSE
Eq 3	-8.17	9.06	-8.65	9.57	-9.02	9.9	-9.13	9.62
Eq 4	9.93	13.09	7.64	11.28	8.15	11.23	10.34	13.88
Eq 5	10.65	13.68	8.33	11.87	8.87	11.84	11.021	14.44
Eq 6	-3.92	5.7	-4.36	6.29	-4.72	6.38	-4.87	5.84
Eq 7	0.49	3.78	0.46	3.7	-0.52	3.99	-0.79	2.94
Eq 11	-14.14	14.77	-14.41	15.12	-15.21	15.68	-14.46	14.88

Tab. 2: Statistical parameters for the validation of several models for estimating LDR. Site 1 (2020-2021). The lowest values are highlighted in red.

SITE 1				
Year	**2020**		**2021**	
Npoints	**1721**		**1376**	
Error(%)	rBias	rRMSE	rBias	rRMSE
Eq 3	-7.04	7.88	-4.72	6.18
Eq 4	14.67	17.736	15.3	18.12
Eq 5	15.27	18.19	15.99	18.69
Eq 6	-2.90	4.87	-0.49	4.37
Eq 7	1.24	3.24	3.7	5.04
Eq 11	-12.58	13.11	-11.29	12.25

Tab. 3: Statistical parameters for the validation of several models for estimating LDR. Site 2 (2020-2021). The lowest values are highlighted in red.

SITE 2				
Year	**2020**		**2021**	
Npoints	**1613**		**1640**	
Error(%)	**rBias**	**rRMSE**	**rBias**	**rRMSE**
Eq 3	-15.87	16.57	-17.69	18.49
Eq 4	-0.96	6.59	0.13	6.22
Eq 5	-0.34	6.53	0.746	6.16

Eq 6	-11.96	12.89	-14.18	15.28
Eq 7	-8.71	9.96	-10.68	11.74
Eq 11	-23.15	23.69	-23.77	24.22

From the statistical parameters presented in tables 1,2, and 3, the performance of the different models evaluated here is consistent between the studied years of one site, however they are not the same if we compare the two sites between them. In site 1, the lowest errors are observed while using the emissivity modeled in equation 7 for all the studied years except for year 2021, while modeling the emissivity using equation 4 and 5 shows the lowest errors for site 2. The observed difference in the calculated errors of the two sites may be due to the fact that the meteorological parameters used in the emissivity model are firstly measured at two different heights between the two sites (at 3m in site 1 and 10 m in site 2), and secondly the AWS in site 2 is a few kilometers away from the main site, which may have introduced some local bias in the comparison between the estimated and measured LDR. Hereafter, we use the data of site 1 to determine the local calcibration for the LDR estimation.

The performance of the models in equations 8 to 10 were also evaluated, however their results are not displayed here since they show high errors. These models have a relation between the emissivity and the ratio e_a/T_a that is similar to the equation determined by Brutsaert in equation 5, but with different coefficients depending on the location where they were derived.

$$\boldsymbol{\varepsilon = C_1 * (\frac{e_a}{T_a})^{C_2}} \qquad \text{(eq 16)}$$

In order to determine the coefficients for the local conditions found in Qatar, we studied in figure 3 the relation between measured LDR and the ratio e_a/T_a, using clear-sky LDR data of year 2015 in site 1. The function found to better fit both was determined, and the two coefficients C_1 and C_2 are obtained from the fit and are shown in the statistics box of figure 3 as p0 and p1, respectively.

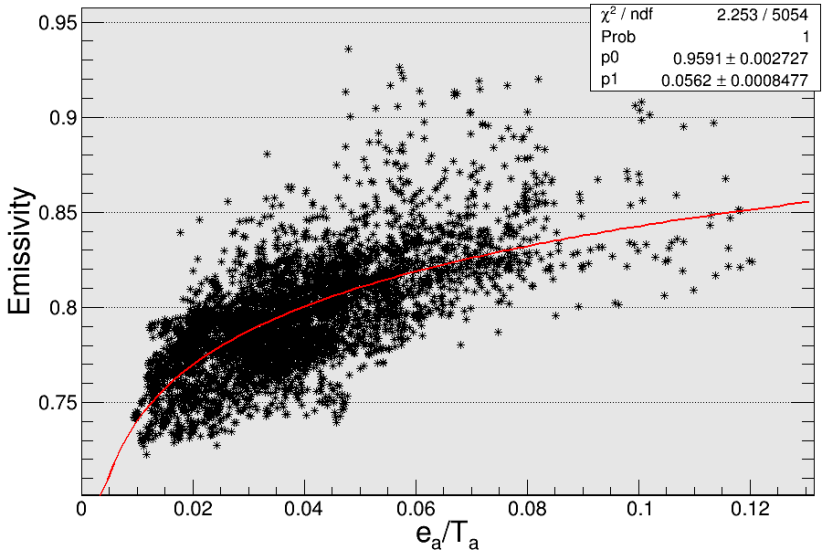

Fig. 3: Correlation between measured LDR and the ratio ea/Ta, using clear-sky LDR data of year 2015 in site 1.

The same local calibration was performed for equation 7 (the best performing model at site 1), using clear-sky LDR data of year 2015 in site 1. In order to determine the coefficients for the local conditions found in Qatar, we determined the function that better fit the data using equation 14; the two coefficients C_3 and C_4 are obtained from the fit and are shown in the statistics box of figure 4 as p0 and p1, respectively.

$$\boldsymbol{\varepsilon = C_3 + C_4 * e_a * \exp(\frac{1500}{T_a})} \qquad \text{(eq 17)}$$

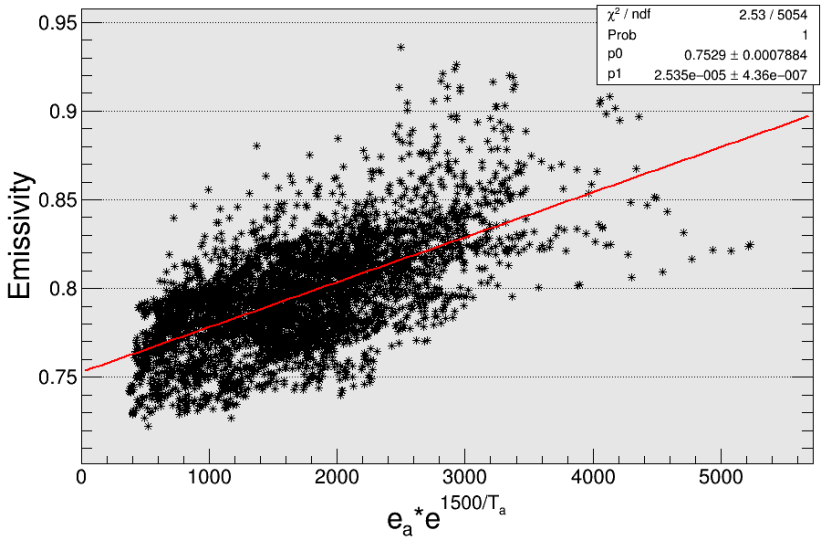

Fig. 4: Correlation between measured LDR and the ratio ea* exp(1500/Ta) using clear-sky LDR data of year 2015 in site 1.

In order to evaluate the performance of the two local models, we used a different dataset than the one used to develop the models. LDR is calculated using equations 15 and 16 and compared with ground measured LDR.

$$\boldsymbol{\varepsilon = 0.959 * (\frac{e_a}{T_a})^{0.0562}} \quad \text{(eq 18)}$$

$$\boldsymbol{\varepsilon = 0.753 + 2.535 * 10^{-5} * e_a * \exp(\frac{1500}{T_a})} \quad \text{(eq 19)}$$

The statistical parameters are displayed in table 4 and show a slight decrease in the error compared to the best performing model for site 1.

Tab. 4: Statistical parameters for the validation of several models for estimating LDR.

Year	2014		2016		2017	
Npoints	**1113**		**1862**		**1052**	
Error(%)	rBias	rRMSE	rBias	rRMSE	rBias	rRMSE
Eq 18	1.03	3.16	-0.06	2.69	0.44	2.44
Eq 19	1.32	3.43	0.16	2.87	0.57	2.54

5. Conclusions

In this contribution, the performance of several models estimating the longwave downward radiation is evaluated against ground measurements in two different locations in Qatar, for 5 years in site 1 and 2 years in site 2. The relative Bias and relative RMSE of the assessment are reported separately for each year. The results show that the models considering both the temperature and water vapour pressure perform better than the models using independently in their empirical relation either the temperature or the water vapor pressure. A local calibration was also performed and local empirical coefficients were determined. The results of the new determined models estimating LDR showed a good performance when validated with 3 years of ground measurements, separately, achieving errors lower than 3.5% with 10-minute resolution data. It is recommended to use these new empirical relations when determining clear-sky LDR in similar atmospheric conditions. A potential continuation of this work will include the validation and calibration of the LDR model under all-sky conditions.

6. References

Brunt, D. 1932. Notes on radiation in the atmosphere. Q. J. R. Meteorol. Soc., 58, 389–420. Doi:10.1002/qj.49705824704

Brutsaert, W. 1975. On a derivable formula for long-wave radiation from clear skies. Water Resour. Res., 11, 742–744. Doi:10.1029/wr011i005p00742

Duarte, H.F., Dias, N.L., Maggiotoo, S.R. 2006. Assessing daytime downward longwave radiation estimates for clear

and cloudy skies in Southern Brazil. Agricultural and Forest Meteorology, 139, 171–181. DOI:10.1016/j.agrformet.2006.06.008

Idso, S.B., Jackson, R. D. 1969. Thermal Radiation From the Atmosphere. J Geophys Res, 74, 5397–5403. DOI:10.1029/JC074i023p05397

Idso, S.B. 1981. A set of equations for full spectrum and 8- to 14-µm and 10.5- to 12.5-µm thermal radiation from cloudless skies. Water Resour. Res. 17, 295–304. DOI:10.1029/WR017i002p00295

Kruk, N.S., Vendrame, I.F., Rocha, H.R., Chou, S.C., Cabral, O. 2010. Downward longwave radiation estimates for clear and all-sky conditions in the Sertãozinho region of São Paulo, Brazil. Theoretical and Applied Climatology, 99, 115–123, 2010. DOI: 10.1007/s00704-009-0128-7

Prata, A.J.A. 1996. A new long-wave formula for estimating downward clear-sky radiation at the surface. Quarterly Journal of the Royal Meteorological Society, 122, 1127–1151. DOI:10.1002/qj.49712253306

Rigollier, C., Bauer, O., Wald, L. 2000. On the clear sky model of the ESRA - European Solar Radiation Atlas with respect to the Heliosat method. Solar Energy, 68 (1), 33-48. DOI:10.1016/S0038-092X(99)00055-9

Sugita, M., Brutsaert, W.H. 1993. Cloud effect in the estimation of instantaneous downward longwave radiation. Water Resources Research, 29, 599–605. DOI:10.1029/92WR02352

Swinbank, W.C. 1963. Long-wave radiation from clear skies. Q. J. R. Meteorol. Soc., 89, 339–348. DOI:10.1002/qj.49708938105

Wagner, W., Pruß. A. 2002. The IAPWS Formulation 1995 for the Thermodynamic Properties of Ordinary Water Substance for General and Scientific Use. Journal of Physical and Chemical Reference Data, 31 (2), 387-535. DOI:10.1063/1.1461829